● termis.

Tissue Engineering
& Regenerative Medicine
International Society

METHODS ARTICLE

Dynamic Bioreactors with Integrated Microfabricated Devices for Mechanobiological Screening

Bogdan M. Beca, MD, MASc,[1] Yu Sun, PhD,[1–3] Edwin Wong, BASc,[1,4]
Christopher Moraes, PhD,[5] and Craig A. Simmons, PhD[1,2,4]

Biomechanical stimulation is a common strategy to improve the growth, maturation, and function of a variety of engineered tissues. However, identifying optimized biomechanical conditioning protocols is challenging, as cell responses to mechanical stimuli are modulated by other multifactorial microenvironmental cues, including soluble factors and biomaterial properties. Traditional bioreactors lack the throughput necessary for combinatorial testing of cell activity in mechanically stimulated engineered tissues. Microfabricated systems can improve experimental throughput, but often do not provide uniform mechanical loading, are challenging to use, lack robustness, and offer limited amounts of cells and tissue for analysis. To address the need for higher-throughput, combinatorial testing of cell activity in a tissue engineering context, we developed a hybrid approach, in which flexible polydimethylsiloxane microfabricated inserts were designed to simultaneously generate multiple tensile strains when stretched cyclically in a standard dynamic bioreactor. In the embodiment presented in this study, each insert contained an array of 35 dog bone-shaped wells in which cell-seeded microscale hydrogels can be polymerized, with up to eight inserts stretched simultaneously in the bioreactor. Uniformity of the applied strains, both along the length of a microtissue and across multiple microtissues at the same strain level, was confirmed experimentally. In proof-of-principle experiments, the combinatorial effects of dynamic strain, biomaterial stiffness, and transforming growth factor (TGF)-β1 stimulation on myofibroblast differentiation were tested, revealing both known and novel interaction effects and suggesting tissue engineering strategies to regulate myofibroblast activation. This platform is expected to have wide applicability in systematically probing combinations of mechanobiological tissue engineering parameters for desired effects on cell fate and tissue function.

Keywords: mechanobiology, bioreactor design, mechanical strain, heart valves, microfabrication, high-throughput screening

Impact Statement

In this study, we introduce a dynamic bioreactor system incorporating microfabricated inserts to enable systematic probing of the effects of combinations of mechanobiological parameters on engineered tissues. This novel platform offers the ease of use, robustness, and well-defined mechanical strain stimuli inherent in traditional dynamic bioreactors, but significantly improves throughput (up to 280 microtissues can be tested simultaneously in the embodiment presented in this study). This platform has wide applicability to systematically probe combinations of dynamic mechanical strain, biomaterial properties, biochemical stimulation, and other parameters for desired effects on cell fate and engineered tissue development.

Introduction

DYNAMIC MECHANICAL FORCES play important regulatory roles in the development, maintenance, and dysfunction of both native and engineered tissues. Mechanical stimula-

tion has been exploited effectively to improve tissue growth, maturation, and function in a number of engineered tissues, including bone, cartilage, liver, lung, smooth muscle, and tendon, with tissue responses sensitive to the magnitude of the applied stress or strain, among other loading parameters.[1–3]

[1]Department of Mechanical and Industrial Engineering, University of Toronto, Toronto, Canada.
[2]Institute of Biomaterials and Biomedical Engineering, University of Toronto, Toronto, Canada.
[3]Department of Electrical and Computer Engineering, University of Toronto, Toronto, Canada.
[4]Translational Biology and Engineering Program, Ted Rogers Centre for Heart Research, University of Toronto, Toronto, Canada.
[5]Department of Chemical Engineering, McGill University, Montreal, Canada.

However, mechanical stimuli act in concert with other microenvironmental cues, including soluble factors, biomaterial properties, and other biophysical stimuli, to direct cell fate and function.[4] Consequently, optimizing conditioning protocols for engineered tissues requires a combinatorial approach that considers the integrative effects of multiple microenvironmental cues.

Traditional bioreactors used to mechanically stimulate engineered tissues lack the throughput necessary to efficiently assess cell and tissue responses to varying levels of mechanical forces or to combinations of microenvironmental cues.[5–7] Developing an understanding of cellular response in this parameter space could serve as a first step in identifying promising combinations of microenvironmental conditions to achieve a desired tissue engineering outcome. To address this need, a variety of miniaturized bioreactors have been proposed to screen combinations of mechanobiological conditions to identify optima for implementation in traditional bioreactors.[8–19] In practice, however, these platforms have yet to realize their full potential for a number of reasons: application of uniform dynamic loading at the microscale is challenging to achieve[8,11,12,14–18,20,21]; throughput remains limited[11,13,15,16,18–20]; oftentimes, a limited number of cells or tissue is available for analysis[8–10,12,13,15,19,20]; and user friendliness and platform robustness remain concerns for routine and nonexpert use.[11,13,16–19]

To enable higher-throughput, combinatorial testing of cell activity in a tissue engineering context, while addressing the limitations of current microdevices, we developed a hybrid approach, in which flexible polydimethylsiloxane (PDMS) microfabricated inserts were designed to simultaneously generate multiple mechanical strains when stretched cyclically in a standard dynamic bioreactor. We focused on cyclic tensile stretch because of its broad relevance to a variety of engineered cardiovascular, orthopedic, and soft connective tissues. In the embodiment presented in this study, eight microfabricated inserts can be subjected to tensile strain in a single bioreactor, with each insert subjected to distinct biochemical conditions. Each insert contains an array of 35 engineered dog bone-shaped cell-seeded hydrogels that are polymerized *in situ*; when stretched in the bioreactor, rows of seven microtissues are subjected to five distinct levels of cyclic tensile strain. Thus, a total of 280 microtissues can be tested, subjected to at least 40 different combinations of mechanical, matrix, and soluble stimuli. To demonstrate the utility of this approach, we probed independent and combined effects of cyclic dynamic strain, biomaterial stiffness, and biochemical stimulation with transforming growth factor (TGF)-β1 on myofibroblast differentiation of valvular interstitial cells (VICs). Myofibroblasts are important for heart valve development, disease, and regeneration,[22–24] and thus an improved understanding of how microenvironmental factors integrate to regulate myofibrogenesis is critical to both understand native valve (patho)biology and identify valve engineering strategies.

Materials and Methods

System design

Our goal was to develop a robust system in which cells and engineered tissues could be subjected to a range of uniform tensile strains, with throughput that enabled combinatorial investigations of mechanical and nonmechanical stimuli. To do so, we designed microfabricated inserts for a dynamic bioreactor, in which arrays of cell-seeded biomaterials could be cultured (Fig. 1a, b). The inserts and engineered tissues cultured on them were then subjected to tensile loading in a standard macroscale dynamic bioreactor (Fig. 1c).

The microfabricated insert was designed to produce five uniform regions of longitudinal strain (Fig. 1a, b). This was achieved through a staircase geometry, whereby successively decreasing substrate thickness produced correspondingly larger strain for a fixed substrate displacement. In this study, we designed inserts that included step thicknesses of 8, 4, 2, 1.33, and 1 mm (Fig. 1a). For an overall longitudinal substrate displacement of 7 mm, these step thicknesses correspond to nominal strain magnitudes of 2.5%, 5%, 10%, 15%, and 20%, respectively. To minimize stress concentrations, corners between steps were filleted with a 1/16″ (1.59 mm) radius.

To provide for replicate samples at each strain level, an array of seven dog bone-shaped microwells (300-μm deep) was patterned on the top of the substrate for each step region (Fig. 1b). The dog bone shape is commonly used in tensile testing since it exhibits uniform longitudinal strain during stretch. To avoid nonuniformities induced by the insert edges or by the change in insert thickness, the microwells were patterned toward the center of each strain region.

The inserts were fabricated from Sylgard 184 PDMS (Dow Corning through Ellsworth Adhesives Canada, Burlington, Canada) through a combination of soft lithography techniques[25] and a modified squeeze fabrication procedure[26,27] (Fig. 2). A 303-stainless steel mold was used to produce the staircase geometry of the substrate and microfabricated SU-8 masters were used to pattern the dog bone-shaped microwells by replica molding. Masters were fabricated by spin coating SU-8 50 (Microchem, Newton, MA) at 1000 rpm on 3″ × 2″ glass slides, after which the slides were prebaked, exposed to ultraviolet (UV) light through a photomask, and postbaked to obtain a thickness of 150 μm. The process was repeated to add a second layer of SU-8 50, after which the slides were developed and hard-baked, achieving a final thickness of 300 μm (the depth of the microwells). Before replica molding, the masters were treated with the mold release silanization agent (Tridecafluoro-1,1,2,2-tetra-hydrooctyl)-1-trichlorosilane (United Chemical Technologies, Bristol, PA), under vacuum.[28] Inserts for static (nonstretched) controls were fabricated by soft lithographically patterning flat PDMS substrates with dog bone microwells in an Omniwell tray lid (Thermo Fisher Scientific, Rochester, NY).

A bioreactor was built to stretch the inserts and thereby subject cell-seeded biomaterials in the dog bone microwells to tensile loading (Fig. 1c). The bioreactor consisted of a sealed enclosure containing four polycarbonate plates (each with two compartments and two clamps), in which two staircase inserts could be mounted, for a total of eight inserts. Cell culture medium was contained separately within each compartment, enabling eight different media conditions to be tested simultaneously. With the insert design reported in this study, all microtissues on a single insert share the same culture medium in one of the compartments.
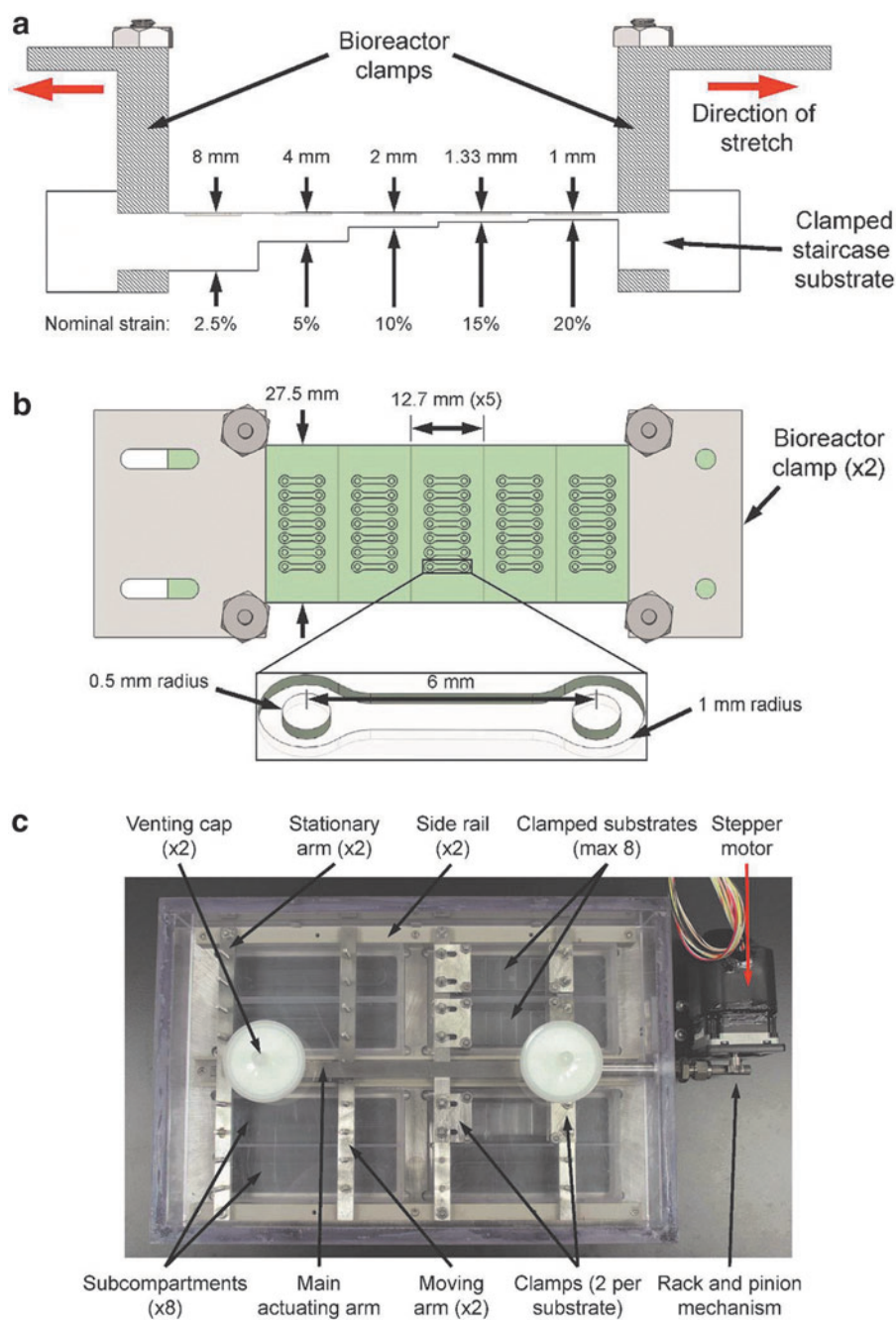
FIG. 1. Overview of integrated microfabricated structures into a conventional mechanically dynamic bioreactor system. **(a)** *Side* cross-sectional view of staircase-profiled inserts to provide multiple strain levels under a single applied stretch. **(b)** *Top* view of staircase inserts showing location and structure of microfabricated dog bone-shaped structures that will be loaded with candidate biomaterials. **(c)** Overview of the bioreactor system, in which eight staircase inserts can be stretched simultaneously to provide a total of 280 microtissues tested under 40 different combinations of mechanical, matrix, and soluble stimuli.

The enclosure was vented to atmosphere through disposable polypropylene venting caps installed on the base (SLFG75010; Thermo Fisher Scientific), which contained a 0.2 μm pore size polytetrafluoroethylene (PTFE) membrane. Each insert was constrained in the bioreactor by two clamps, one bolted to stationary arms and the other to moving arms. The stationary arms were bolted to a pair of side rails and the moving arms were welded to the main actuating arm, which was connected to an actuation rod that served as the rack for a rack-and-pinion-type actuating mechanism. The actuating rod was guided through the chamber by a PTFE sleeve bearing and the actuating arm was constrained to the longitudinal stretch direction by linear sliders. To reduce friction during motion, the moving arms ran along two side rails that were made of polyether ether ketone and lubricated with Vaseline. The actuation mechanism consisted of a high torque NEMA-23 stepper motor (HT23-399; Applied Motion, Watsonville, CA), which was environmentally sealed, mounted with a pinion (S10T05M021S0505; Stock Drive Products/Sterling Instrument, New Hyde Park, NY) that connected to the actuation rod custom fitted with a rack (S181YYM0508200; Stock Drive Products/Sterling Instrument). The motor could be connected to a personal computer and programmed for desired loading patterns through a programmable step motor driver (Si2035; Applied Motion). The bioreactor and motor were designed to be moved as a single intact unit from the incubator to a biological safety cabinet for sterile medium changes, which were done
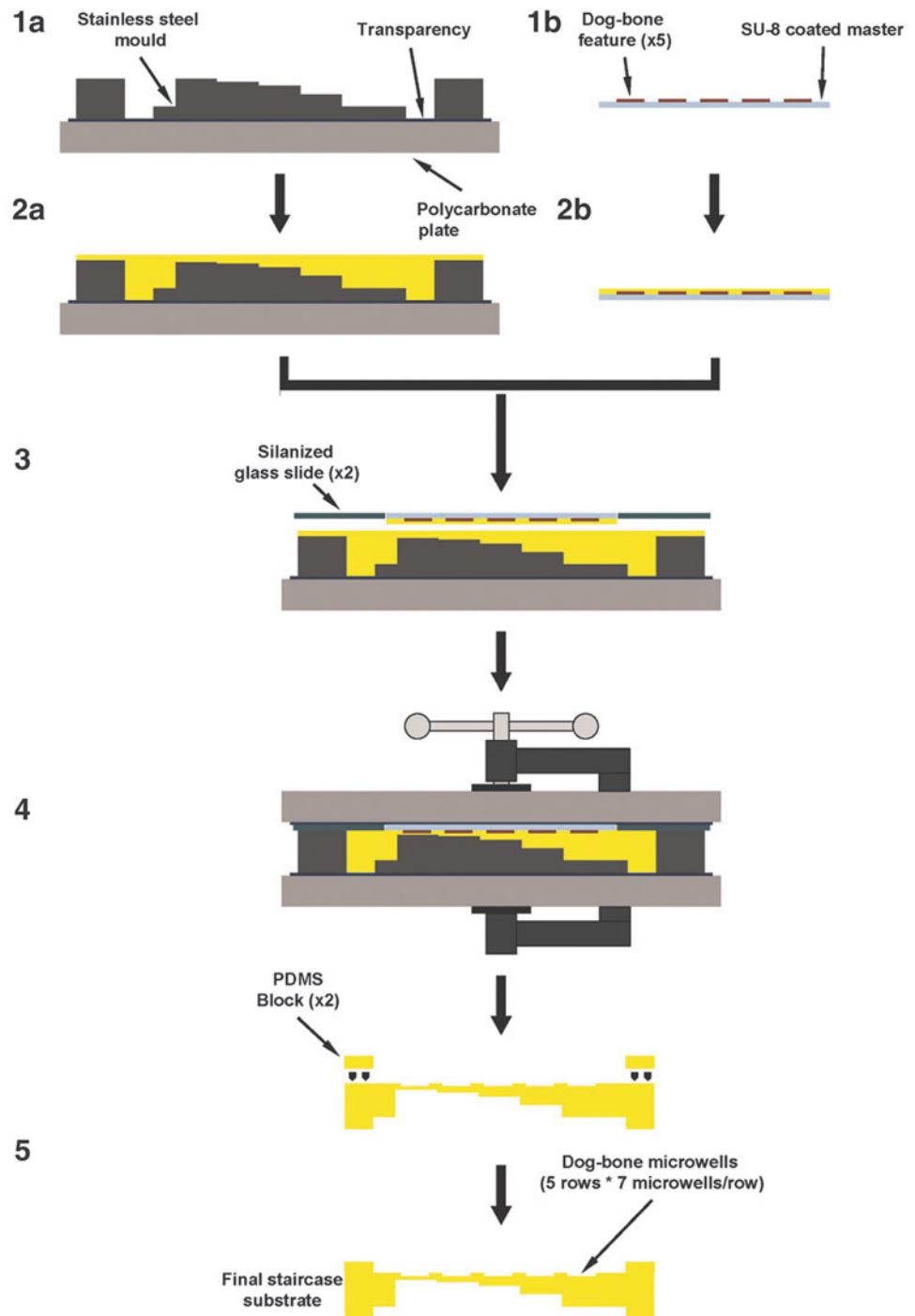
FIG. 2. Schematic of staircase substrate fabrication process. (Step 1a) A stainless steel mold was used to create the staircase geometry (shown in Fig. 1a), whereas (Step 1b) a SU-8 master was used to create the dog bone-shaped microwells (shown in Fig. 1b). (Step 2a, b) Molds were filled with PDMS (*yellow*), and (Step 3) combined by inverting the SU-8 well master on top of the stainless steel staircase mold, with silanized glass slides placed on either side of the SU-8 master to produce the end regions for clamping. (Step 4) The entire assembly was sandwiched between transparencies and polycarbonate plates, clamped, and thermally cured to produce a monolithic PDMS structure. (Step 5) The substrate was removed from the mold and PDMS blocks were bonded to the substrate ends to produce the final substrate that can be clamped in the bioreactor. PDMS, polydimethylsiloxane.

by disengaging the actuating rod from the rack and moving the rod slightly into the chamber to remove the lid and exchange medium in each compartment by pipetting. To make medium changes less laborious, a future improvement to the chamber design would be to include capped access ports in the lid for direct access to each chamber.

Hydrogel fabrication and integration into inserts

To demonstrate the utility of the bioreactor system, gelatin methacrylate (gelMA) was used as a model biomaterial as it has been shown to support cell adhesion and proliferation,[29–31] including VICs,[32,33] and it can be micropatterned through photopolymerization. It also has tunable mechanical properties, which can improve mechanical integrity under loading compared to collagen gels, and enables study of substrate stiffness effects (a potent stimulus for VICs[18,22,34,35]).

gelMA was synthesized as described previously.[29] Briefly, gelatin from porcine skin (Sigma-Aldrich Canada Ltd., Oakville, Canada) was dissolved in phosphate-buffered saline (PBS) without Ca^{2+}/Mg^{2+} at 50°C and stirred for 30 min until fully dissolved. Methacrylic anhydride (94%; Sigma-Aldrich Canada Ltd.) at 8% (volume/volume) was

added to the solution at a rate of 0.5 mL/min under stirred conditions and allowed to react for 3 h at 50°C. The pH of the solution was monitored throughout and was kept at pH = 5 by adding a few drops of 5 M NaOH solution, when necessary. After a 3x dilution with PBS, the reaction was stopped and the solution was dialyzed against deionized water at 50°C for 1 week. The solution was then filtered, lyophilized for another week, and stored dry at room temperature until use.

To prepare gelMA hydrogels, Irgacure 2959 [2-hydroxy-1-(4-(hydroxyethoxy)phenyl]-2-methyl-1-propanone (Ciba Specialty Chemicals, Inc., Basel, Switzerland) was used as a photoinitiator and dissolved at 2% (weight/volume) concentration in PBS at 80°C for 20 min. The gelMA precursor was then dissolved in the photoinitiator solution at 80°C for 20 min at 8.5 wt % or 20 wt %, corresponding to elastic moduli of 6 or 33 kPa measured as described previously.[33] The solution was then poured over the empty microwells of the oxygen plasma-treated PDMS staircase substrates, excess gelMA was removed, and the gelMA was UV photocrosslinked (Blak-Ray Model B 100AP lamp; UVP, Upland, CA) for 225 s (8.5 wt %) or 150 s (20 wt %). Polymerized gelMA did not bind to the PDMS surface, but is retained in the dog bone-shaped inserts by the integrated micropillars, which apply tensile strain to the tissues when the devices are stretched. Substrates patterned with gelMA were stored in PBS and used for strain characterization studies or were seeded with primary porcine aortic VICs, as described below. While not tested in this study, cells alternatively could be mixed within a hydrogel precursor and polymerized in a three-dimensional (3D) seeded configuration directly in the microwells, as described above.

Insert and hydrogel strain characterization

The staircase inserts were designed to achieve nominal strain values based on a one-dimensional (1D) theoretical model that does not account for large deformations and geometric features like fillets that could affect the actual strain levels achieved. To better characterize the strains across the inserts for each step region, a geometrically accurate 3D model was generated using SolidWorks 2010 (Dassault Systèmes SolidWorks Corp., Waltham, MA) and was analyzed by the finite element (FE) method using ANSYS 13.0 (ANSYS, Inc., Canonsburg, PA). The FE model consisted of 20-node solid elements (SOLID186), with the PDMS modeled as a linear elastic material with large deformations. Displacement boundary conditions were applied as in the bioreactor: the fixed clamp end was constrained from movement in all directions, and the moving clamp end was subjected to axial *x*-direction displacement, but constrained in the orthogonal directions. An overall axial displacement of 7 mm was applied to the insert. FE engineering strains were computed within the microwells from the position of the center of every microwell post before and after stretch.

To validate the FE predictions, axial microwell strains were measured in each strain region by measuring the relative displacement of the centers of the microwell posts before and after stretch (7 mm overall substrate displacement) from digital images obtained with a Navitar high-magnification (12×) zoom lens (Navitar, Rochester, NY) and a high-resolution IEEE1394 digital black and white camera (Sony, Vienna, Austria).

Strain transfer from the inserts to the hydrogels was characterized by measuring axial strain in the middle "shaft" region of the dog bone-shaped hydrogel samples, where strains were predicted to be uniform. To do so, tissue-marking dye (Triangle Biomedical Sciences, Inc., Durham, NC) was dotted on the surface of the gels using a toothpick. Axial hydrogel strains were determined from the relative displacement of pairs of dots at the ends of the straight region of the hydrogel dog bones during stretching. To quantify strain uniformity, higher resolution images of the dots were taken; axial and transverse strains for each dot along the shaft region were calculated using the relative change in dot length during stretching (Supplementary Fig. S1). All images were analyzed with ImageJ (NIH).

Cell mechanobiological stimulation experiments

Primary VICs were isolated from aortic heart valves of pigs from a local abattoir (Quality Meat Packers, Toronto, Canada) as reported previously.[35] Cells were cultured in Dulbecco's Modified Eagle Medium supplemented with 10% fetal bovine serum and 1% penicillin/streptomycin solution and used after one passage. For the stretching experiments reported in this study, VICs were seeded at 7500 cells/cm^2 on gelMA hydrogels that had been polymerized in wells on the staircase inserts. Cell-seeded hydrogel arrays were incubated at 37°C for 48 h to allow for attachment and spreading before being clamped in the bioreactor.

The combinatorial effects of dynamic stretch, substrate stiffness, and biochemical stimulus on VIC myofibroblast differentiation were probed in a single experiment using four staircase substrates (half of the bioreactor capacity). Two substrates were molded with low stiffness gels (6 kPa) and the remaining two with high stiffness gels (33 kPa), representing normal and early fibrotic valve tissue, respectively. Immediately before stretching, one substrate from each pair was treated with 5 ng/mL of TGF-β1. The staircase inserts were then cyclically stretched at 1 Hz for 48 h with 7 mm overall substrate displacement to achieve nominal strains of 2.5%, 5%, 10%, 15%, and 20% for the respective steps on the substrates. A duplicate set of substrates was maintained under static conditions. This full set of experiments was repeated four times with independent cell populations. Once the experiments concluded, cells were fixed with 10% neutral buffered formalin, permeabilized with 0.1% Triton X-100, and immunostained for α-smooth muscle actin (SMA; Cy3-conjugated mouse anti-SMA clone 1A4), F-actin (FITC-labeled phalloidin), and cell nuclei (1 ng/mL Hoechst 33342). Imaging was performed with a fluorescent microscope (Model IX71; Olympus, Center Valley, PA) connected to a camera (Model Retiga 2000R; Qimaging, Surrey, Canada). Image analysis was conducted in ImageJ (NIH) to quantify the percentage of myofibroblasts in a cell population following previously described methods,[11] in which SMA incorporation into stress fibers was used to identify myofibroblasts.

Statistical analyses

SigmaStat 3.5 (Systat Software, Inc., San Jose, CA) was used for all statistical tests. Multiway analyses of

variance (ANOVA) were used as appropriate, with pairwise comparisons by the Student-Newman-Keuls test. To test the dependency of SMA on strain, stiffness, and TGFB-β1, a three-way ANOVA was used, with main and interaction effects reported. Planned pairwise comparisons between selected test conditions were conducted by t-tests based on recommended guidelines for multifactorial data analysis t-tests.[36] Data are expressed as mean ± standard deviation.

Results

Microwell strain characterization in inserts

As expected, the microwell axial strains determined by the FE method were similar to those predicted by the simplified 1D strain model, and matched the empirically observed strains measured on the hydrogel surface (Fig. 3a and Supplementary Fig. S2). Axial strains measured for each microwell in a single strain region were consistent within the same strain region, but distinct from microwells located in other strain regions (Fig. 3b; $p < 0.001$). The coefficient of variability between the six independent inserts tested was <4%, indicating excellent sample-to-sample consistency. Thus, the stretched inserts generate five statistically distinct strain levels, with seven equivalent replicates at each strain level and good consistency between independent inserts.

Hydrogel strain characterization

We next characterized axial strains in hydrogels within the substrate microwells, considering both 6 and 33 kPa hydrogels (three substrates per modulus), as strain transfer from substrate to hydrogel may be influenced by the hydrogel stiffness. Deformation in both 6 and 33 kPa hydrogels was distinct in the separated strain regions, but the stiffer gels ruptured during stretching at the largest strains tested (20%), and therefore, data for this condition are not available for comparison (Fig. 4a, b). Hydrogel strains were generally consistent with observed deformation of the PDMS microwells, with only slight variations at high and low strains. As with the insert microwell strains, hydrogel strains differed significantly between discrete strain regions ($p < 0.001$), but not between microwells within the same region ($p > 0.13$) for both 6 and 33 kPa hydrogels (Fig. 4c, d). As expected, due to Poisson's effects, the hydrogels also experienced transverse strains that were approximately half the magnitude of the axial strain in each discrete strain region (Supplementary Fig. S3).

We evaluated strain homogeneity along the length of the hydrogel dog bone by measuring axial strain at four dot locations in shaft of the dog bone in the middle of each strain region (sample No. 4 in Fig. 4c, d). We found that there were no significant differences in axial strain between the four dot locations on individual dog bones for both the 6 kPa ($p = 0.77$; Fig. 4e)

FIG. 3. **(a)** Average microwell axial strains measured in each strain region of the staircase substrates were comparable to those predicted by finite element analyses and generally slightly below nominal strains based on a simplified 1D analytical model. **(b)** PDMS microwell axial strains within steps were not statistically different, but increased significantly across substrate steps. Results are presented as mean ± standard deviation (**$p < 0.05$ and $n = 6$ substrates). 1D, one dimensional.
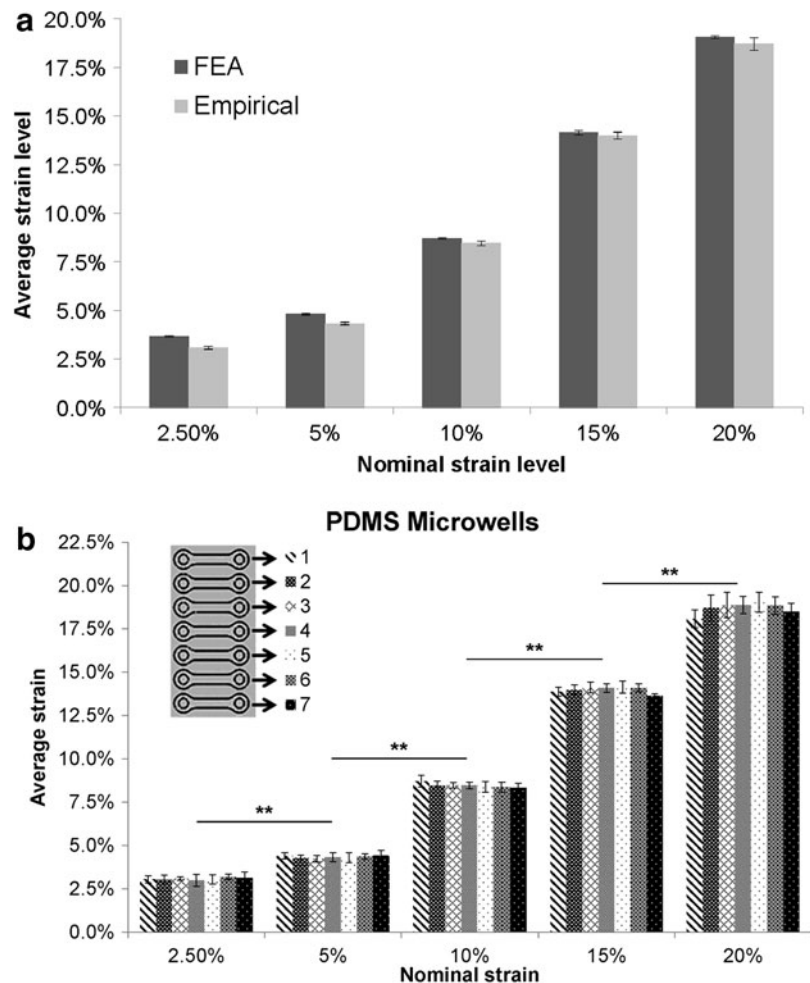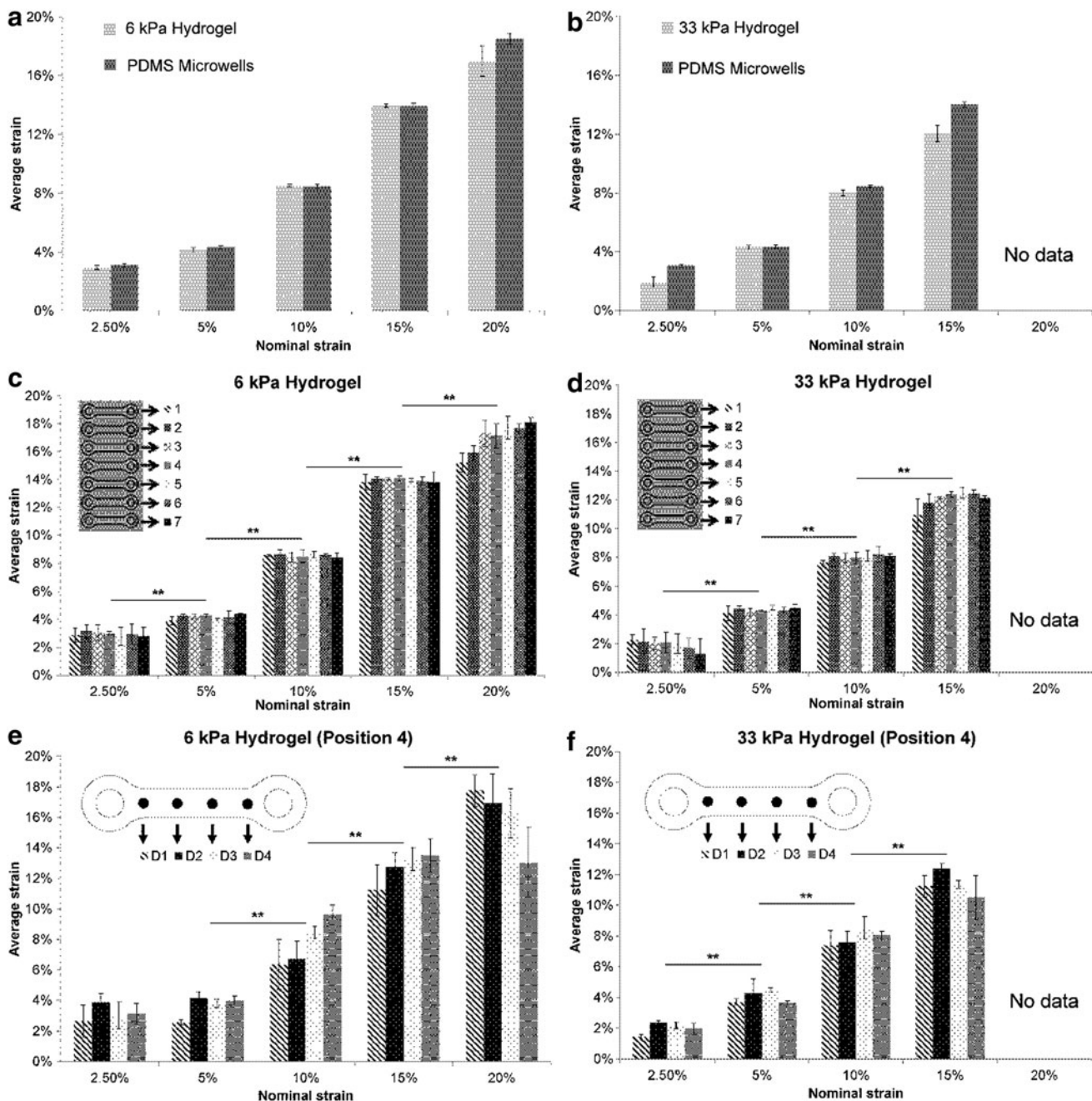
FIG. 4. Axial strains measured on **(a)** 6 kPa and **(b)** 33 kPa hydrogels within the microwells were not significantly different from those of the microwells, although the 33 kPa gels ruptured at 20% applied strain. Axial strains for the **(c)** 6 kPa and **(d)** 33 kPa hydrogel dog bones within each strain step were not significantly different, but differed significantly between distinct strain regions. Finally, strains were homogeneous along the length of a dog bone at all measured strain levels for both the **(e)** 6 kPa and **(f)** 33 kPa hydrogels. Results are presented as mean ± standard deviation (**$p < 0.01$ and $n = 3$ substrates per stiffness).

and 33 kPa ($p = 0.11$; Fig. 4f) hydrogels. Thus, hydrogels in the stretched inserts undergo deformation at five statistically distinct strain levels, with seven equivalent replicates at each strain level and homogeneity along the length of the shaft regions.

SMA expression as a function of gel stiffness, strain magnitude, and biochemical treatment

Finally, to demonstrate the utility of the bioreactor system, we evaluated the combined effects of cyclic strain magnitude (static controls, 2.5%, 5%, 10%, or 15% nominal strains; 20% strains were not considered because the 33 kPa hydrogels ruptured), hydrogel stiffness (6 or 33 kPa), and biochemical treatment (0 or 5 ng/mL TGF-β1) on VIC myofibroblast differentiation, as assessed by proportion of cells expressing SMA in the uniform strain shaft regions. The throughput of the substrates and bioreactor enabled us to do this in a single experiment, with seven replicates per condition, using only half of the bioreactor capacity. While the seven replicates could be assigned for

different assays, we used them in this study as technical replicates for immunostaining and repeated the experiment four times. Analysis by a three-way ANOVA revealed main effects of strain ($p < 0.001$) and TGF-β1 treatment ($p < 0.001$), but not stiffness ($p = 0.14$) on the proportion of myofibroblasts (Fig. 5). In addition, there was a significant interaction effect between strain and TGF-β1 treatment ($p = 0.030$), but nonsignificant interactions between stiffness and strain ($p = 0.071$), stiffness and TGF-β1 ($p = 0.83$) treatment, and the three factors together ($p = 0.81$) in the context of this experiment. Notably, dynamic strain had no significant effect in the absence of TGF-β1 treatment for either stiffness (Fig. 5a–c; $p > 0.05$). However, with TGF-β1 treatment and for both gel stiffnesses, dynamic strain up 10% increased the myofibroblast proportion in a dose-dependent manner, with significant differences over static culture at most strain levels (Fig. 5a, b, d; $p < 0.05$).

Discussion

Including mechanical force stimulation in bioreactors for tissue engineering applications is a well-established technique to improve tissue formation metrics. However, identifying the precise combination of biological and mechanical culture conditions that drive cells toward a desired phenotype in a tissue is challenging due to limited throughput in conventional bioreactors, and practical challenges of robustness and utility in more advanced microengineered screening platforms. To address this issue, we adopt a hybrid approach that uses microfabricated inserts to increase throughput, while a conventional bioreactor system applies the driving force to mechanically deform the culture. Varying the thickness of the sample in a ''staircase'' geometry was used to generate multiple strains across the microfabricated insert, enabling 40 independent conditions with 7 replicates per condition for multiple assays. Furthermore, the system allows the rapid and simple integration of customized 3D cell-laden hydrogels, to determine how matrix properties direct cell function under cyclic mechanical stretch, demonstrating that the modularity of this hybrid bioreactor/microfabricated insert approach can readily enable a broad range of parametric tests when appropriately designed.

For the cyclic linear strain system designed and tested in this study, strains transferred well from the PDMS microwells to both the 6 and 33 kPa hydrogels, and were consistent across replicates within each strain region (Figs. 3b, 4c, and 4d). The stiff 33 kPa hydrogels did rupture at high strains, but this is a characteristic of the specific gelMA material system used in this study. This issue can be avoided by limiting strain applied, or utilizing one of several high-toughness tissue engineering materials[37–39] as the matrix of interest for specific applications.

The strains were reasonably homogenous across each hydrogel construct, but did show some small variations (Fig. 4e, f). These minor variations may be caused by vertical slippage of the hydrogel along the anchoring pillars, which could be alleviated by micromolding overhanging structures on the anchoring pillars as has been previously demonstrated.[40] Despite the minor strain variations observed, observed strains are close to the expected strain levels for each strain region, and distinct from strains in other regions of the microfabricated insert, enabling strain ''dose dependency'' to be conveniently tested in a single insert.

As a test case for the system, we screened combinations of mechanical strain (0–15%), hydrogel stiffness (6 vs. 33 kPa), and biochemical treatment (±TGF-β1) for their combined effects on myofibroblast differentiation of VICs. VICs exhibit significant phenotypic plasticity in response to microenvironmental stimuli,[41] and activation of myofibroblasts is a key step in valve development, disease, and regeneration.[42] Thus, insights into how myofibroblast activation can be modulated by microenvironmental cues are of broad interest, including for defining biomaterial properties and mechanobiological stimulation protocols to engineer heart valve tissues.[43] In one-factor-at-a-time studies, VIC myofibroblast differentiation has been shown to increase with mechanical strain,[11,34,44] on stiffer substrates,[35,45–47] and with TGF-β1 treatment.[35,41,46] Notably, in the context of multiple mechanobiological stimuli as tested in this study, we found VIC myofibroblast differentiation to be significantly promoted by dynamic strain and TGF-β1 treatment, but not stiffness (Fig. 5). The lack of dependency on stiffness is particularly interesting, as several studies suggest a threshold substrate stiffness for VIC activation to myofibroblasts of ~15 kPa, at least under static conditions.[35,48]

FIG. 5. **(a)** The bioreactor system was used to probe the combinatorial effects of cyclic strain, hydrogel stiffness, and TGF-β1 treatment on myofibroblast differentiation of valve interstitial cells, quantified as the proportion of total cells (counterstained with Hoechst nuclear label; *blue*) expressing α-smooth muscle actin-positive stress fibers (*red*). Three-way ANOVA identified significant main effects of strain ($p < 0.001$) and TGF-β1 treatment ($p < 0.001$) and a significant interaction effect of strain and TGF-β1 treatment ($p = 0.03$), but no significant main or interaction effects involving hydrogel stiffness. Pairwise comparisons for the effects of strain on **(b)** 6 kPa and **(c)** 33 kPa gels with (*red lines*) and without (*black lines*) TGF-β1 treatment revealed significantly more myofibroblasts, with the application of strain only in the presence of TGF-β1. *Red asterisks* indicate significant difference ($p < 0.05$) relative to 0% (static) condition for the TGF-β1(+) conditions. *Black asterisks* indicate significant differences ($p < 0.05$) with and without TGF-β1 treatment at specific strain levels. Similarly, **(d)** without exogenous TGF-β1 treatment, there was no significant effect of strain stimulation on myofibroblast differentiation, regardless if the cells were on 6 kPa (*blue*) or 33 kPa (*black*) hydrogels. **(e)** With TGF-β1 treatment, the proportion of myofibroblasts increased with strain stimulation equivalently for both stiffnesses, with the only difference being that there were more myofibroblasts on the 33 kPa hydrogels (*black*) than on the 6 kPa hydrogels (*blue*) under static conditions. *Blue* and *black asterisks* indicate significant difference ($p < 0.05$) relative to 0% (static) condition for the 6 and 33 kPa conditions, respectively. *Gray asterisk* indicates significant differences ($p < 0.05$) between 6 and 33 kPa conditions at 0% strain. All results are presented as mean ± standard deviation for three to four experimental replicates. ANOVA, analyses of variance; TGF, transforming growth factor.
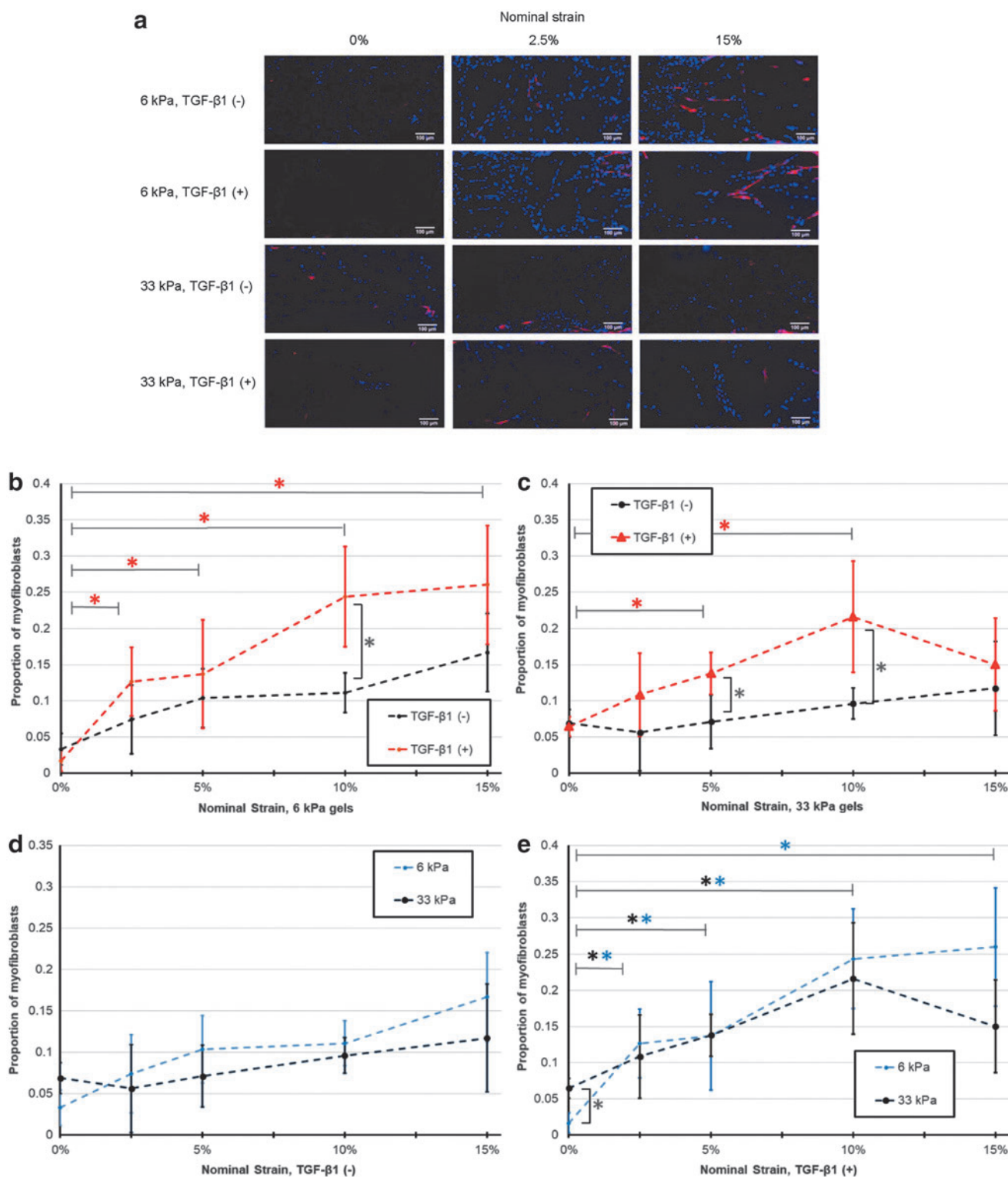
Indeed, in this study, we observed significantly more myofibroblasts on the 33 kPa gels than on the 6 kPa gels under static conditions with TGF-β1 treatment ($p < 0.05$; Fig. 5d). However, when subjected to dynamic strain, VICs activated on 6 kPa gels to the same extent as on 33 kPa gels, suggesting that externally applied strain can compensate for low matrix stiffness to drive myofibroblast differentiation (Fig. 5d). This novel observation extends that of Throm Quinlan *et al.*,[49]

who found that VICs were rounded on 0.3 kPa gels, but when subjected to short-term strain (10%, 6 h), spread equivalently to VICs on 50 kPa gels. In the context of valve tissue engineering, these results suggest a mechanism to temporally control myofibroblast activation by using external strain to activate and static culture to deactivate, as long as the gels are sufficiently soft. However, our results indicate that robust myofibroblast differentiation by mechanical

stimulation can only occur in the presence of TGF-β1 (Fig. 5c, d). This observation of synergism between strain and TGF-β1 to promote VIC myofibroblast differentiation is consistent with previous reports[11,34] and identifies another mechanism to regulate myofibroblast activation in engineered valve and other connective tissues.

While this system addresses some of the issues with existing miniaturized bioreactors, including enabling well-characterized, uniform dynamic loading across a range of strains and increasing throughput in a facile manner, there remain some limitations. First, the platform is best suited for biomaterials that can be polymerized directly in the PDMS substrates. While dog bone-shaped scaffolds fabricated off substrate could be loaded in theory, this would undermine the throughput advantages offered by the system. Second, the relatively small size of the microtissues may limit the types of molecular and biochemical analyses that can be performed, as only up to hundreds of cells can be loaded at typical 3D seeding densities. Furthermore, mechanical testing of recovered microtissues would be limited to microscale/nanoscale techniques like indentation because of their small size. Third, all 35 microtissue samples on a single substrate are contained within the same compartment in this design, and as such, all microtissues on a substrate share the same culture medium. This could potentially result in paracrine signaling between microtissues at different strain levels, although these confounding effects would be expected to be minimized by dilution by the large medium volumes in each compartment, the relatively small number of cells, and the relatively large distances between microtissues at each strain level. To eliminate any potential for cross-contamination between microtissues, the PDMS substrates could be modified to include wells on their surface to isolate each microtissue or row of microtissues at the same strain level. Fourth, although the system has been demonstrated to perform well with gelMA as the matrix material, validation experiments would be required for alternative tissue materials, particularly for those that might form adhesions to PDMS, which could introduce strain heterogeneity as the tissues remodel.

In summary, we report the design and manufacture of a bioreactor system for high-throughput combinatorial screening of cell and engineered tissue responses to multiple mechanobiological stimuli, including mechanical tension, matrix stiffness, and biochemical factors. The system consists of a bioreactor vessel in which flexible PDMS substrates patterned with microwells containing cell-seeded hydrogels can be stretched longitudinally to subject up to 280 microtissues to at least 40 different combinations of mechanical, matrix, and soluble stimuli in a single experiment. Capitalizing on the throughput afforded by this system, the combinatorial effects of dynamic strain, biomaterial stiffness, and TGF-β1 stimulation on myofibroblast differentiation were tested, revealing both known and novel interaction effects and suggesting tissue engineering strategies to regulate myofibroblast activation. Similarly, this platform should have wide applicability to systematically probe other combinations of mechanobiological culture parameters for their effects on cell fate and tissue function.

Supplementary Material

Supplementary Figure S1
Supplementary Figure S2
Supplementary Figure S3

References

1. Moraes, C., Mehta, G., Lesher-Perez, S.C., and Takayama, S. Organs-on-a-chip: a focus on compartmentalized microdevices. Ann Biomed Eng **40**, 1211, 2012.
2. Riehl, B.D., Park, J.H., Kwon, I.K., and Lim, J.Y. Mechanical stretching for tissue engineering: two-dimensional and three-dimensional constructs. Tissue Eng Part B Rev **18**, 288, 2012.
3. Mihic, A., Li, J., Miyagi, Y., et al. The effect of cyclic stretch on maturation and 3D tissue formation of human embryonic stem cell-derived cardiomyocytes. Biomaterials **35**, 2798, 2014.
4. Discher, D.E., Mooney, D.J., and Zandstra, P.W. Growth factors, matrices, and forces combine and control stem cells. Science **324**, 1673, 2009.
5. Langer, R., and Vacanti, J.P. Tissue engineering. Science **260**, 920, 1993.
6. Khademhosseini, A., Langer, R., Borenstein, J., and Vacanti, J.P. Microscale technologies for tissue engineering and biology. Proc Natl Acad Sci U S A **103**, 2480, 2006.
7. Lei, Y., and Ferdous, Z. Design considerations and challenges for mechanical stretch bioreactors in tissue engineering. Biotechnol Prog **32**, 543, 2016.
8. Tremblay, D., Chagnon-Lessard, S., Mirzaei, M., Pelling, A.E., and Godin, M. A microscale anisotropic biaxial cell stretching device for applications in mechanobiology. Biotechnol Lett **36**, 657, 2014.
9. Maeda, E., Hagiwara, Y., Wang, J.H., and Ohashi, T. A new experimental system for simultaneous application of cyclic tensile strain and fluid shear stress to tenocytes in vitro. Biomed Microdevices **15**, 1067, 2013.
10. Park, S.H., Sim, W.Y., Min, B.H., Yang, S.S., Khademhosseini, A., and Kaplan, D.L. Chip-based comparison of the osteogenesis of human bone marrow- and adipose tissue-derived mesenchymal stem cells under mechanical stimulation. PLoS One **7**, e46689, 2012.

11. Moraes, C., Likhitpanichkul, M., Lam, C.J., Beca, B.M., Sun, Y., and Simmons, C.A. Microdevice array-based identification of distinct mechanobiological response profiles in layer-specific valve interstitial cells. Integr Biol (Camb) **5,** 673, 2013.

12. Wang, Q., Zhang, X., and Zhao, Y. Micromechanical stimulator for localized cell loading: fabrication and strain analysis. J Micromech Microeng **23,** 015002, 2013.

13. Moraes, C., Wang, G., Sun, Y., and Simmons, C.A. A microfabricated platform for high-throughput unconfined compression of micropatterned biomaterial arrays. Biomaterials **31,** 577, 2010.

14. Tan, W., Scott, D., Belchenko, D., Qi, H.J., and Xiao, L. Development and evaluation of microdevices for studying anisotropic biaxial cyclic stretch on cells. Biomed Microdevices **10,** 869, 2008.

15. Shimizu, K., Shunori, A., Morimoto, K., Hashida, M., and Konishi, S. Development of a biochip with serially connected pneumatic balloons for cell-stretching culture. Sens Actuators B Chem **156,** 486, 2011.

16. Kamotani, Y., Bersano-Begey, T., Kato, N., *et al.* Individually programmable cell stretching microwell arrays actuated by a Braille display. Biomaterials **29,** 2646, 2008.

17. Simmons, C.S., Sim, J.Y., Baechtold, P., *et al.* Integrated strain array for cellular mechanobiology studies. J Micromech Microeng **21,** 54016, 2011.

18. Moraes, C., Chen, J.H., Sun, Y., and Simmons, C.A. Microfabricated arrays for high-throughput screening of cellular response to cyclic substrate deformation. Lab Chip **10,** 227, 2010.

19. Moraes, C., Zhao, R., Likhitpanichkul, M., Simmons, C.A., and Sun, Y. Semi-confined compression of microfabricated polymerized biomaterial constructs. J Micromech Microeng **21,** 2011.

20. Huang, J.W., Pan, H.J., Yao, W.Y., *et al.* Interaction between lung cancer cell and myofibroblast influenced by cyclic tensile strain. Lab Chip **13,** 1114, 2013.

21. Kim, T.K., and Jeong, O.C. Fabrication of a pneumatically-driven tensile stimulator. Microelectron Eng **98,** 715, 2012.

22. Yip, C.Y., and Simmons, C.A. The aortic valve microenvironment and its role in calcific aortic valve disease. Cardiovasc Pathol **20,** 177, 2011.

23. Butcher, J.T., Mahler, G.J., and Hockaday, L.A. Aortic valve disease and treatment: the need for naturally engineered solutions. Adv Drug Deliv Rev **63,** 242, 2011.

24. Hinz, B., Phan, S.H., Thannickal, V.J., Galli, A., Bochaton-Piallat, M.L., and Gabbiani, G. The myofibroblast—one function, multiple origins. Am J Pathol **170,** 1807, 2007.

25. Xia, Y.N., and Whitesides, G.M. Soft lithography. Annu Rev Mater Sci **28,** 153, 1998.

26. Moraes, C., Sun, Y., and Simmons, C.A. Solving the shrinkage-induced PDMS alignment registration issue in multilayer soft lithography. J Micromech Microeng **19,** 065015, 2009.

27. Jo, B.H., Van Lerberghe, L.M., Motsegood, K.M., and Beebe, D.J. Three-dimensional micro-channel fabrication in polydimethylsiloxane (PDMS) elastomer. J Microelectromech Syst **9,** 76, 2000.

28. Anderson, J.R., Chiu, D.T., Jackman, R.J., *et al.* Fabrication of topologically complex three-dimensional micro-fluidic systems in PDMS by rapid prototyping. Anal Chem **72,** 3158, 2000.

29. Nichol, J.W., Koshy, S.T., Bae, H., Hwang, C.M., Yamanlar, S., and Khademhosseini, A. Cell-laden microengineered gelatin methacrylate hydrogels. Biomaterials **31,** 5536, 2010.

30. Aubin, H., Nichol, J.W., Hutson, C.B., *et al.* Directed 3D cell alignment and elongation in microengineered hydrogels. Biomaterials **31,** 6941, 2010.

31. Hutson, C.B., Nichol, J.W., Aubin, H., *et al.* Synthesis and characterization of tunable poly(ethylene glycol): gelatin methacrylate composite hydrogels. Tissue Eng Part A **17,** 1713, 2011.

32. Benton, J.A., DeForest, C.A., Vivekanandan, V., and Anseth, K.S. Photocrosslinking of gelatin macromers to synthesize porous hydrogels that promote valvular interstitial cell function. Tissue Eng Part A **15,** 3221, 2009.

33. Chen, M.B., Srigunapalan, S., Wheeler, A.R., and Simmons, C.A. A 3D microfluidic platform incorporating methacrylated gelatin hydrogels to study physiological cardiovascular cell-cell interactions. Lab Chip **13,** 2591, 2013.

34. Merryman, W.D., Lukoff, H.D., Long, R.A., Engelmayr, G.C., Jr., Hopkins, R.A., and Sacks, M.S. Synergistic effects of cyclic tension and transforming growth factor-beta1 on the aortic valve myofibroblast. Cardiovasc Pathol **16,** 268, 2007.

35. Chen, J.H., Chen, W.L., Sider, K.L., Yip, C.Y., and Simmons, C.A. Beta-catenin mediates mechanically regulated, transforming growth factor-beta1-induced myofibroblast differentiation of aortic valve interstitial cells. Arterioscler Thromb Vasc Biol **31,** 590, 2011.

36. Keppel, G., and Wickens, T.D. Design and Analysis: A Researcher's Handbook. Upper Saddle River, NJ: Pearson Prentice Hall, 2004.

37. Sun, G., Li, Z., Liang, R., Weng, L.T., and Zhang, L. Super stretchable hydrogel achieved by non-aggregated spherulites with diameters <5 nm. Nat Commun **7,** 12095, 2016.

38. Shi, F.K., Wang, X.P., Guo, R.H., Zhong, M., and Xie, X.M. Highly stretchable and super tough nanocomposite physical hydrogels facilitated by the coupling of intermolecular hydrogen bonds and analogous chemical crosslinking of nanoparticles. J Mater Chem B **3,** 1187, 2015.

39. Sun, J.Y., Zhao, X., Illeperuma, W.R., *et al.* Highly stretchable and tough hydrogels. Nature **489,** 133, 2012.

40. Legant, W.R., Pathak, A., Yang, M.T., Deshpande, V.S., McMeeking, R.M., and Chen, C.S. Microfabricated tissue gauges to measure and manipulate forces from 3D microtissues. Proc Natl Acad Sci U S A **106,** 10097, 2009.

41. Chester, A.H., and Taylor, P.M. Molecular and functional characteristics of heart-valve interstitial cells. Philos Trans R Soc Lond B Biol Sci **362,** 1437, 2007.

42. Rabkin-Aikawa, E., Farber, M., Aikawa, M., and Schoen, F.J. Dynamic and reversible changes of interstitial cell phenotype during remodeling of cardiac valves. J Heart Valve Dis **13,** 841, 2004.

43. Parvin Nejad, S., Blaser, M.C., Santerre, J.P., Caldarone, C.A., and Simmons, C.A. Biomechanical conditioning of tissue engineered heart valves: too much of a good thing? Adv Drug Deliv Rev **96,** 161, 2016.

44. Balachandran, K., Konduri, S., Sucosky, P., Jo, H., and Yoganathan, A.P. An ex vivo study of the biological properties of porcine aortic valves in response to circumferential cyclic stretch. Ann Biomed Eng **34,** 1655, 2006.
45. Yip, C.Y., Chen, J.H., Zhao, R., and Simmons, C.A. Calcification by valve interstitial cells is regulated by the stiffness of the extracellular matrix. Arterioscler Thromb Vasc Biol **29,** 936, 2009.
46. Pho, M., Lee, W., Watt, D.R., Laschinger, C., Simmons, C.A., and McCulloch, C.A. Cofilin is a marker of myofibroblast differentiation in cells from porcine aortic cardiac valves. Am J Physiol Heart Circ Physiol **294,** H1767, 2008.
47. Wang, H., Haeger, S.M., Kloxin, A.M., Leinwand, L.A., and Anseth, K.S. Redirecting valvular myofibroblasts into dormant fibroblasts through light-mediated reduction in substrate modulus. PLoS One **7,** e39969, 2012.
48. Kloxin, A.M., Benton, J.A., and Anseth, K.S. In situ elasticity modulation with dynamic substrates to direct cell phenotype. Biomaterials **31,** 1, 2010.
49. Throm Quinlan, A.M., Sierad, L.N., Capulli, A.K., Firstenberg, L.E., and Billiar, K.L. Combining dynamic stretch and tunable stiffness to probe cell mechanobiology in vitro. PLoS One **6,** e23272, 2011.

Address correspondence to:
Christopher Moraes, PhD
Department of Chemical Engineering
McGill University
M.H. Wong Building, Room 4330
3610 University Street
Montreal, QC H3A 0C5
Canada

E-mail: chris.moraes@mcgill.ca

Craig A. Simmons, PhD
Translational Biology and Engineering Program
Ted Rogers Centre for Heart Research
University of Toronto
661 University Ave, 14th floor
Toronto, ON M5G 1M1
Canada

E-mail: c.simmons@utoronto.ca